Intramolecular Electron Transfer across Amino Acid Spacers in the Picosecond Time Regime. Charge−Transfer Interaction through Peptide Bonds 1

ARTICLE · JANUARY 1999

DOI: 10.1021/jp9832802

8 AUTHORS, INCLUDING:

David Gosztola
Argonne National Laboratory
129 PUBLICATIONS **4,638** CITATIONS

Intramolecular Electron Transfer across Amino Acid Spacers in the Picosecond Time Regime. Charge-Transfer Interaction through Peptide Bonds[1]

Guilford Jones II,* Lily N. Lu, Hongning Fu, Catie W. Farahat, and Churl Oh

Department of Chemistry and the Center for Photonics, Boston University, Boston Massachusetts 02215

Scott R. Greenfield,[†] David J. Gosztola,[†] and Michael R. Wasielewski*,[†,‡]

Chemistry Division, Argonne National Laboratory, Argonne, Illinois 60439, and Department of Chemistry, Northwestern University, Evanston Illinois 60208

Received: August 5, 1998; In Final Form: November 23, 1998

For a series of alanine-based peptides having 1−3 amino acid residues as spacers, the chromophore, pyrenesulfonyl (Pyr), has been attached at the N-terminus and an electron donor, dimethyl-1,4-benzenediamine (DMPD), covalently bound at the C-terminus. Evidence for an intramolecular charge-transfer interaction involving the electron donor and acceptor groups has been obtained from absorption spectra. Intramolecular electron transfer involving the end groups, Pyr (electron acceptor) and DMPD (electron donor) has been confirmed by ultrafast pump−probe methods. The radical-ion pair states that are generated on Ti/sapphire laser excitation at 400 nm decay in the picosecond to nanosecond time domain and generally show multiexponential decay kinetics. These rates of charge recombination are among the fastest yet observed involving electron transfer between terminal groups for peptide oligomers. The falloff of rate constants for ion pair recombination is irregular in terms of the through-bond distance that separates Pyr and DMPD groups for the various peptide links; i.e., back electron transfer remains fast for the tripeptide, Pyr-Ala-Ala-Ala-DMPD, despite an average through-bond distance between photoactive groups that reaches 18 Å. Molecular modeling studies show that the peptides are free to adopt conformations in essentially random fashion, without showing evidence for long range ordering of the peptide chain.

Introduction

Over the past decade a number of structures have been prepared having electron donor and acceptor groups that are covalently bound to peptide oligomers.[2−6] Principal objectives of this work have encompassed the elucidation of the role of amino acid linkages in providing either a relatively rigid framework for the systematic placement of donor and acceptor groups at a varying distance of separation or the assembly of potential electron-transfer reactants in larger peptide assemblies (e.g., the scaffolding of an α-helix). For several series involving synthetic peptides that are substituted with non-native organic or transition metal groups or with native reactive side chains (e.g., tyrosine or tryptophan),[2−7] time constants for electron transfer in the nanosecond to millisecond domain have been observed (generally, a range of rate constants, $k = 10^3-10^8$ s^{-1}). Peptide links have featured prominently the amino acid proline,[2−4] a residue that provides a relatively rigid link having limited conformational possibilities for pendant groups.

The assumption made in most electron-transfer studies involving peptides is that the connecting amino acid residues are not electroactive (i.e., not involved in discrete electron-transfer steps). The peptide links play a more subtle role in which electron-transfer rates vary with the number of amino acid residues in an intervening peptide linkage. Although there are interesting variations (vide infra), a general finding is a falloff in the rate of photoinduced electron transfer with distance for A-spacer-D peptides that supports a mechanism of electronic coupling involving the peptide chain (an approximate exponential dependence on through-bond distance in accord with theoretical models[8]). In a more general context, the results provide some insight with regard to the role of amino acid linkages in large *de novo* peptide assemblies (e.g., "bundles") and in proteins for which electron transport is important.[9,10]

In this paper a new series of synthetic peptides (**2**−**4**) is reported that employs one of the simplest amino acids, L-alanine (Ala), as a spacer. The amine terminal group of alanine or a short peptide sequence is modified by attachment of a chromophore, the pyrenesulfonyl group (Pyr), a moiety that also serves as an electron acceptor. The C-terminal group of the spacer is further modified by placement of an electron donor group, *N*,*N*-dimethyl-1,4-benzenediamine (DMPD), as the carboxamide derivative. These peptides provide another assessment of the roles of structure and electron-transfer dynamics having three distinct features. Compared to the oligoproline links (**6**), the alanine oligomers are free to adopt a larger variety of conformations and represent, to a greater degree, the conformational dispersion found more generally for peptide chains. In addition, we have focused in this study on the observation of phototransients and rates of *charge recombination*; the result is an assessment of peptide electron-transfer behavior for the Marcus "inverted region" (for a thermodynamic driving force, $\Delta G_{et} < -2.0$ eV). The values determined using ultrafast laser flash methods are among the fastest yet measured for electron transfer along a peptide chain (for the series, **2**−**4**, dominant decay constants fall in the 10−100 ps domain). Also of value

[†] Argonne National Laboratory.
[‡] Northwestern University.

10.1021/jp9832802 CCC: $18.00
Published on Web 12/31/1998

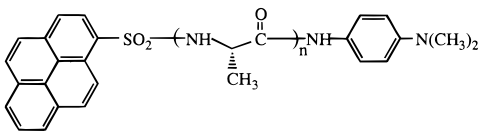

1 n = 0, Pyr-DMPD

2 n = 1, Pyr-Ala-DMPD

3 n = 2, Pyr-Ala-Ala-DMPD

4 n = 3, Pyr-Ala-Ala-Ala-DMPD

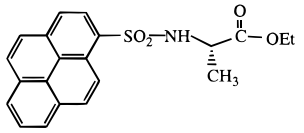

5 Pyr-AlaOEt

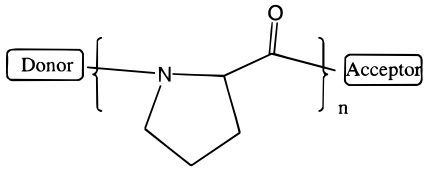

6

for this series is the finding that the strength of electronic coupling involving interaction of the remotely placed Pyr and DMPD groups can be evaluated qualitatively through the observation of weak charge-transfer bands that contribute to absorption spectra.

The systems reported are analogous to others in which a simple aromatic chromophore (usually the hydrocarbon moiety, pyrene, serving as electron acceptor) has been used in conjunction with peptides that have been conjugated with aromatic amines as electron donors.[5] In these complementary studies, the novel rate effects that have been reported have been restricted to the forward electron-transfer step (as in eq 1) in which a

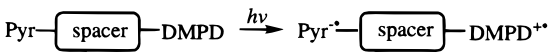

(1)

remotely placed amine donor donates an electron to a photoexcited pyrene, an event that is normally monitored through observation of pyrene fluorescence quenching. The objective of the present work was to highlight the charge recombination step and to attempt to sort out some of the complexities that attend examination of systems that display conformational freedom.

Experimental Section

Materials. The preparation of Pyr-AlaOEt (**5**) has been previously described.[7] The benzyloxycarbonyl-protected amino acids were obtained from Bachem Bioscience Inc., and the amino acid ethyl esters from Sigma. *N*,*N*-Dimethylbenzene-1, 4-diamine (DMPD) (Aldrich) was freshly distilled at 0.1 mmHg pressure (bp ca. 100 °C) under an argon atmosphere before use. Acetonitrile, dioxane (HPLC grade, Fisher), and dimethylformamide (DMF) (<0.005% water, Aldrich) were used as received.

Peptide Coupling Methodology and General Procedures. Traditional methods for solution-phase coupling of amino acids were employed by following general steps[11] that include protection at the N-terminus with the benzyloxycarbonyl group (Cbz), activation of the carboxylic acid group with nitrophenol, and coupling of the amino and carboxylic acid groups using the diimide reagent, DCC. Silica gel 60 (230−400 mesh, E. Merck Inc.) was employed as the stationary phase for flash column chromatography (typically 2.5 cm i.d. × 32 cm for a 0.5−1.0 g sample of crude product) with a gradient of petroleum ether−ethyl acetate as typical elution solvent.

***N*-Acetyl-*N*′,*N*′-dimethylbenzene-1,4-diamine (Ac-DMPD).** Freshly distilled *N*′,*N*′-dimethylbenzene-1,4-diamine (DMPD) (5.0 g, 0.038 mol) was dissolved in 30 mL of Ar-purged pyridine in the dark. On addition of acetic anhydride (3.7 mL, 3.9 g, 0.038 mol), the reaction mixture was refluxed at 80 °C for 30 min. The pH of the cooled solution was adjusted to 7.0 by adding 2.0 N NaOH. The resulting solution was extracted with ethyl ether (3 × 50 mL), the organic extracts were washed with 5% HCl, 5% Na_2CO_3, and water successively and then dried over Na_2SO_4. Removal of solvent in vacuo gave a solid that was recrystallized from benzene/petroleum ether to yield 5.5 g of off-white crystals (81%) (mp 134−135 °C). ^{1}H NMR (400 MHz, CD_3CN): δ 8.22 (br, D−N*H*), 7.32 (d, J = 10.0 Hz, D−H-2, D−H-6), 6.67 (d, J = 9.0 Hz, D−H-3, D−H-5), 2.84 (s, D−N(C*H*$_3$)$_2$), 2.00 (s, C*H*$_3$−C═O). HRMS (EI 70 eV): *m*/*z* 178.1114 (M^+, calcd for $C_{10}H_{14}N_2O$ 178.1106).

***N*-(1-Pyrenesulfonyl)-*N*′,*N*′-dimethylbenzene-1,4-diamine (Pyr-DMPD).** 1-Pyrenesulfonyl chloride[12] (0.50 g, 1.7 mmol) was dissolved in 15 mL of THF and 2 mL of triethylamine. *N*,*N*-Dimethylbenzene-1, 4-diamine (0.24 g, 1.7 mmol, freshly distilled) in 3 mL of THF was added dropwise with stirring. The reaction was stirred at room temperature for 12 h. The precipitate was filtered off and the solvent removed by rotary evaporation, yielding a brownish yellow solid. The solid was purified by flash column chromatography on silica gel and recrystallized from ethyl acetate/petroleum ether to yield 0.21 g (30%) of orange needles (mp 175−177 °C): ^{1}H NMR (400 MHz, CD_3COCD_3): δ 9.12 (d, J = 9.4 Hz, H-10), 8.92 (br, D−N*H*), 8.53 (d, J = 8.3 Hz, H-2), 8.45 (d, J = 7.7 Hz, H-8), 8.43 (d, J = 7.7 Hz, H-6), 8.38 (d, J = 9.4 Hz, H-9), 8.33 (d, J = 9.0 Hz, H-5), 8.27 (d, J = 8.3 Hz, H-3), 8.21 (d, J = 9.0 Hz, H-4), 8.18 (t, J = 7.7 Hz, H-7), 6.83 (d, J = 9.1 Hz, D−H-2, D−H-6), 6.39 (d, J = 9.1 Hz, D−H-3, D−H-5), 2.83 (s, D−N(C*H*$_3$)$_2$). HRMS (EI 70 eV): *m*/*z* 400.1194 (M^+, calcd for $C_{24}H_{20}N_2O_2S$ 400.1246).

***N*-[*N*-(1-Pyrenesulfonyl)-L-alanyl]-*N*′,*N*′-dimethylbenzene-1,4-diamine (Pyr-Ala-DMPD).** Benzyloxycarbonyl-L-alanine-*p*-nitrophenyl ester (2.5 g, 7.3 mmol) was dissolved in 25 mL of pyridine, and the solution was cooled to 0 °C. *N*,*N*-Dimethylbenzene-1,4-diamine (0.99 g, 7.3 mmol, freshly distilled) in 10 mL pyridine was added dropwise, and the reaction was stirred at 0 °C for 2 h and at room temperature overnight. The solvent was removed by rotary evaporation and the resulting solid washed with ethyl ether to yield 1.9 g (77%) of a light yellow precipitate (mp 184−186 °C). A mixture of the product, *N*-benzyloxycarbonyl-L-alanyl-*N*′,*N*′-dimethylbenzene-1,4-diamine (Cbz-Ala-DMPD, 0.60 g, 1.8 mmol), in 10 mL of 80% acetic acid and 0.06 g of Pd/C (10%) hydrogenation catalyst was stirred under hydrogen provided by a balloon for 24 h. The Pd/C was filtered and the solvent removed by rotary evaporation to yield a solid that was washed with ethyl ether to give 0.44 g (92%) of a white precipitate (mp 123−125 °C). The resulting acetate salt of *N*-(L-alanyl)-*N*′,*N*′-dimethylbenzene-1,4-diamine

(0.36 g, 1.3 mmol) was dissolved in a pyridine/methanol mixture (1:1 v/v) along with 2 mL of triethylamine. 1-Pyrenesulfonyl chloride (0.50 g, 1.8 mmol) in 5 mL of pyridine was added dropwise, and the reaction was stirred at room temperature for 12 h. The solvent was removed by rotary evaporation, and the product was purified by flash column chromatography on silica gel (ethyl acetate and petroleum ether gradient). The solid was recrystallized from ethyl acetate/petroleum ether to yield 0.14 g (23%) of orange crystals (mp 198−199 °C): ^{1}H NMR (400 MHz, CD_3COCD_3): δ 9.23 (d, J = 9.4 Hz, H-10), 8.81 (d, J = 8.2 Hz, H-2), 8.69 (br, D−N*H*), 8.56 (d, J = 7.6 Hz, H-8), 8.55 (d, J = 7.6 Hz, H-6), 8.54 (d, J = 9.4 Hz, H-9), 8.43 (d, J = 8.2 Hz, H-3), 8.41 (d, J = 8.9 Hz, H-5), 8.30 (t, J = 7.6 Hz, H-7), 8.30 (d, J = 8.9 Hz, H-4), 7.35 (d, J = 8.3 Hz, A−N*H*), 6.97 (d, J = 9.1 Hz, D−H-2, D−H-6), 6.42 (d, J = 9.1 Hz, D−H-3, D−H-5), 4.15 (m, A−C*H*), 2.95 (s, D−N(CH_3)$_2$), 1.31 (d, J = 7.0 Hz, A−CH_3). HRMS (EI, 70 eV): *m*/*z* 471.1602 (M^+, calcd for $C_{27}H_{25}N_3O_3S$ 471.1617).

***N*-[*N*-(1-Pyrenesulfonyl)-L-alanyl-L-alanyl]-*N*′,*N*′-dimethylbenzene-1,4-diamine (Pyr-Ala-Ala-DMPD).** Following a procedure similar to that for preparation of Pyr-Ala-DMPD, the *N*-benzyloxycarbonyl-L-alanyl-L-alanine-*p*-nitrophenyl ester (white solid, mp 163−164 °C, 60%) was first prepared from *N*-benzyloxycarbonyl-L-alanyl-L-alanine (2.4 g, 8 mmol) and *p*-nitrophenol (1.1 g, 8 mmol) using DCC coupling. Subsequent condensation with *N*,*N*-dimethylbenzene-1,4-diamine provided Cbz-Ala-Ala-DMPD (mp 245−247 °C), which was subjected to catalytic hydrogenration (10% Pd/C), as described. The resulting acetate salt of *N*-(L-alanyl-L-alanyl)-*N*′,*N*′-dimethylbenzene-1,4-diamine (0.45 g, 1.3 mmol) was allowed to react with 1-pyrenesulfonyl chloride (0.54 g, 1.8 mmol). The product was purified by recrystallization three times from ethyl acetate to yield 0.12 g (17%) of light yellow needles (mp 251.0−251.5 °C): ^{1}H NMR (400 MHz, CD_3COCD_3): δ 9.11 (d, J = 10 Hz, H-10), 8.76 (br, D−N*H*), 8.72 (d, J = 7.6 Hz, H-2), 8.47 (d, J = 8.0 Hz, H-8), 8.46 (d, J = 8.0 Hz, H-6), 8.44 (d, J = 10 Hz, H-9), 8.42 (d, J = 7.6 Hz, H-3), 8.38 (d, J = 8.4 Hz, H-5), 8.28 (d, J = 8.4 Hz, H-4), 8.21 (t, J = 8.0 Hz, H-7), 7.56 (d, J = 6.8 Hz, A_2−N*H*), 7.41 (d, J = 9.2 Hz, D−H-2, D−H-6), 7.33 (br, A_1−N*H*), 6.67 (d, J = 9.2 Hz, D−H-3, D−H-5), 4.16 (m, A_2−C*H*), 3.92 (m, A_1−C*H*), 2.85 (s, D−N(CH_3)$_2$), 1.14 (d, J = 6.8 Hz, A_2−CH_3), 1.03 (d, J = 7.6 Hz, A_1−CH_3). HRMS (EI, 70 eV): *m*/*z* 542.1959 (M^+, calcd for $C_{30}H_{30}N_4O_4S$ 542.1977).

***N*-[*N*-(1-Pyrenesulfonyl)-L-alanyl-L-alanyl-L-alanyl]-*N*′,*N*′-dimethylbenzene-1,4-diamine (Pyr-Ala-Ala-Ala-DMPD).** According to the manual solid-phase procedure of Stewart and Young[11] a support resin, 1% cross-linked polystyrene, was functionalized by chloromethylation for reaction with N-protected amino acid. For the pyrene-labeled tripeptide, the 1-pyrenesulfonyl group is coupled with the aminoacyl resin in THF in the presence of triethylamine in the last cycle. The product was cleaved from the resin using anhydrous HF, and the solution of free peptide was washed with anhydrous ether. The free C-terminal peptide was directly coupled with DMPD, and the final product purified by reversed-phase HPLC. Materials used in solid-phase peptide coupling included Boc-amino acid resin esters and Boc-amino acids obtained from Peninsula Laboratories. Preparative HPLC separation of the tripeptide utilized a Dynamax-60 C-18 reversed-phase column and a gradient mobile phase of acetonitrile and water (12 mL/min flow rate); Pyr-Ala-Ala-Ala-DMPD was obtained as a light yellow crystal (yield 30% − 40%, based on available amino acid residues on the resin) (mp > 300 °C): ^{1}H NMR (400 MHz, DMSO-d_6) δ 9.55 (s, D-NH), 8.99 (d, J = 9.4 Hz, H-10), 8.58 (d, J = 8.0 Hz, H-2), 8.52 (d, J = 8.4 Hz, A_1−NH), 8.48 (d, J = 7.4 Hz, H-8), 8.46 (d, J = 7.4 Hz, H-6), 8.42 (d, J = 9.4 Hz, H-9), 8.38 (d, J = 8.0 Hz, H-3), 8.38 (d, J = 8.9 Hz, H-5), 8.28 (d, J = 8.9 Hz, H-4), 8.21 (t, J = 7.4 Hz, H-7), 7.39 (d, J = 7.9 Hz, A_2−NH), 7.82 (d, J = 7.8 Hz, A_3−NH), 7.33 (d, J = 8.6 Hz, D−H-2, D−H-6), 6.65 (d, J = 8.6 Hz, D−H-3, D−H-5), 4.24 (m, A_3−CH). 3.92 (m, A1-CH), 3.79 (m, A_2−CH), 3.33 (s, D−N(CH$_3$)2), 1.17 (d, J = 6.9 Hz, A_3−CH$_3$), 0.98 (d, J = 6.9 Hz, A_1−CH$_3$), 0.81 (d, J = 6.9 Hz, A_2−CH$_3$). HRMS (EI, 70 eV): *m*/*z* 613.2360 (M^+, calcd for $C_{33}H_{35}N_5O_5S$ 613.2359).

General Methods and Procedures. Steady-state emission spectra were recorded using a PTI QuantaMaster Luminescence spectrometer model SE-900M. For fluorescence quantum yield measurements,[13] argon-purged solutions in 1 × 1 cm quartz cells were used (OD < 0.2 at the excitation wavelength); the reference was coumarin 1 (Φ_f = 1.0, CH_3CN). The oxidation potentials for $CH_3CONHC_6H_4N(CH_3)_2$ (Ac-DMPD) and for **1** (first oxidation wave) ($E_{1/2}$ = 0.53 and 0.56 V vs SCE, respectively) and the reduction potential for Pyr-AlaOEt (**5**) ($E_{1/2}$ = −1.69 V vs SCE) were determined by cyclic voltammetry using an EG&G Princeton Applied Research model 273 potentiostat/galvanostat, a platinum bead working electrode, and a platinum wire working electrode. Reversible waves were observed for nitrogen-purged acetonitrile solutions (22 °C) with 0.1 M $LiClO_4$ and scan rates of 0.2−10 V/s.

Ultrafast Transient Detection. The femtosecond transient absorption apparatus consists of a self-mode-locked Ti/sapphire oscillator that produces 25 fs pulses at 97 MHz. The oscillator ouput was temporally stretched in a single grating pulse stretcher, then amplified in a 23 kHz Ti:sapphire regenerative amplifier that is pumped by an intracavity frequency-doubled, Q-switched, Nd:YAG laser. Seeding and subsequent ejection of the amplified pulse was accomplished with a 2 mm quartz acousto-optic modulator (NEOS) with a carrier wave that is both phase and frequency locked to 4 times that of the oscillator (388 Hz). Both the pulse stretcher and compressor utilize quadruply passed holographic transmission gratings (Kaiser Optical). The pulse stretcher utilizes a one-to-one inverting telescope, whereas the compressor's telescope is noninverting.[14] The compressed, amplified output was split and 80% was frequency-doubled to serve as the pump beam.

Samples were typically 10 mM, held in a stirred, 1 cm cuvette, and excited with 0.5 μJ, 70 fs, 400 nm pulses. The remaining 20% of the amplified 800 nm light was used to generate a white-light continuum probe by focusing into a 2 mm sapphire window. The probe beam was polarized at the magic angle (54.7°) with respect to the pump beam. Amplified photodiodes were used to detect single wavelengths of the probe light, after it passed through a computer-controlled monochromator (SPEX model 270M). The photodiode outputs were digitized and recorded using a personal computer. Multiexponential fits of the kinetic data were determined using nonlinear least-squares analysis based on the Leven−Marquardt algorithm.

Molecular Modeling. The software employed was based on QUANTA from Molecular Simulations, Inc.[15] It included the conformational search subroutine that interfaces with the CHARMm molecular mechanics program. Additionally, a semiempirical quantum mechanical program, MOPAC (version 6.0; QCPE 455), was used in determining charge distributions. To arrive at an array of low-energy (most probable) conformations for a particular peptide, the sequence of steps began with a random selection of all the flexible dihedral angles. The

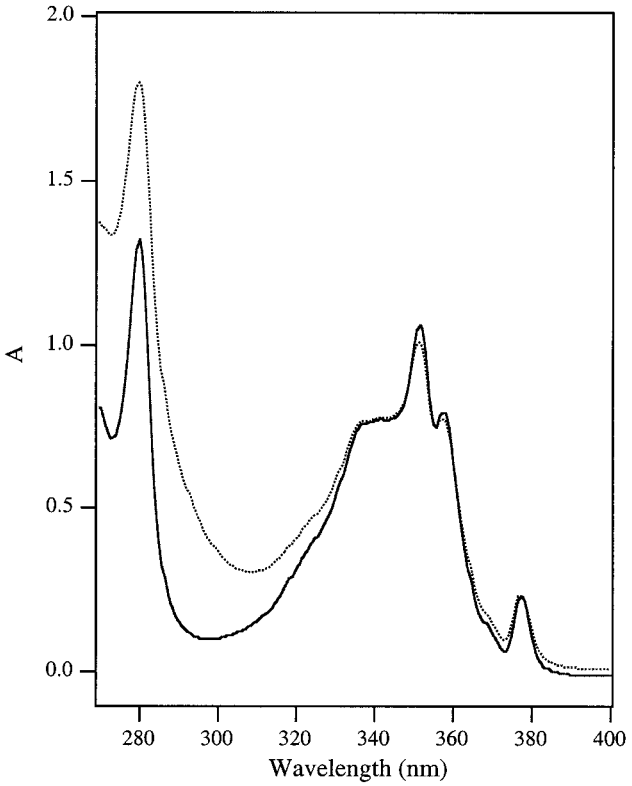

Figure 1. Absorption spectra for **2** and **5**, 30 μM in DMF.

resulting high-energy conformation was energy-minimized by the adopted-basis Newton−Raphson algorithm. For these computations, the solvent dielectric constant was assumed to be that of DMF (36.7) and to be radial-distance-dependent; the amide carbonyl and amide proton positions were assumed to be antiparallel and coplanar.

Results

Absorption and Fluorescence Properties of Peptide Conjugates. For the series **1**−**4**, features in common with the pyrenesulfonamide chromophore attached to the amino acid, alanine, were observed; the conjugate, Pyr-AlaOEt (**5**), absent in the DMPD donor group, was available for comparison.[7] Principal maxima appeared at 278 and 350 nm (for **5**, ϵ = 44 100, and 34 900 M^{-1} cm^{-1}, respectively) with enhancements at 280−310 nm for conjugates bearing the DMPD group (Figure 1). Also, for these DMPD conjugates, a very weak tail intruded into the visible region just past 400 nm. The extent of this long wavelength absorption depended on chain length, suggesting that a perceptible (and variable) interaction was important for Pyr and DMPD acceptor−donor moieties and operates at relatively long range. Relevant also was the observation that the DMPD conjugates were lightly colored as crystalline solids—orange for **1** and **2** and light yellow for **3** and the tripeptide, Pyr-Ala-Ala-Ala-DMPD (**4**).

The anticipated charge-transfer interaction[16,17] between electron acceptor and donor groups in **1**−**4** was examined in more detail with expansion of the absorption data in the 400−500 nm region. The spectra that result for **1** and for oligomeric peptides are shown in Figure 2; these absorption tails were not the result of an aggregation phenomenon since the absorption of solutions having varied concentrations of the conjugates obeyed Beer's law. In no case did the weak charge-transfer (CT) absorptions appear as well resolved bands, but approximate extinction coefficients corresponding to an estimated maximum

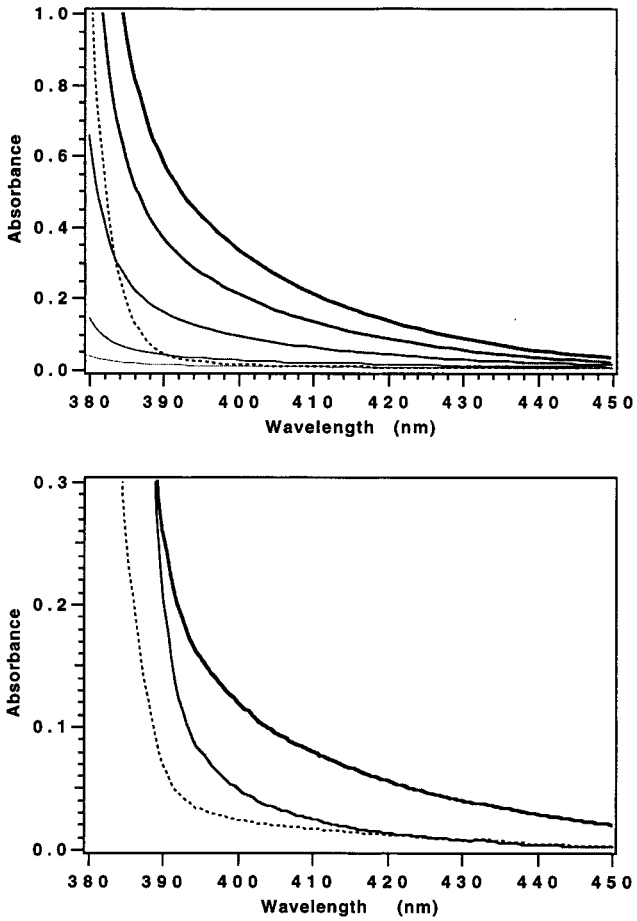

Figure 2. Long wavelength absorption assigned to contribution of a charge-transfer band for **1** (solid lines, concentration increasing, 0.013, 0.063, 0.12, 0.33, and 0.53 mM) and for model compound **5** (dashed line, 0.53 mM) (top) and for 0.53 M conjugates **2** (thick line), **3** (thin line), and **5** (dashed line) (bottom).

for the CT band at 410 nm could be obtained for the two shortest links: 302 (**1**) and 110 (**2**) M^{-1} cm^{-1}. For this approximation, the CT bands were constructed as Gaussian functions (Figure 3), using long wavelength portions of the absorption bands for the DMPD conjugates after subtraction of absorption by Pyr-AlaOEt (**5**) to provide the long wavelength portion of the Gaussian fit. Using the relationship derived by Mulliken and Hush (eq 2),[18,19] it was possible to evaluate the electronic

$$H_{ab}\,(cm^{-1}) = \frac{2.06 \times 10^{-2}\,(\nu_{max}\epsilon_{max}\Delta\nu_{1/2})^{1/2}}{r_{ab}} \qquad (2)$$

coupling matrix elements (H_{ab}) associated with the interaction of Pyr and DMPD groups. The interaction energies obtained using this approximate procedure were 609 (**1**) and 225 (**2**) cm^{-1}. Although the CT bands were not sufficiently defined for **3** and **4**, one could estimate that for these peptides, $\epsilon_{410} = < 30$ M^{-1} cm^{-1} ($H_{ab} < 60$ cm^{-1}). For the Mulliken−Hush relation, ν_{max} and $\Delta\nu_{1/2}$ correspond to the frequency of the reconstructed CT band maxima and bandwidths at half-height, respectively, ϵ is the extinction coefficient for peak CT absorption, r_{ab} is the distance of separation (through bonds, from sulfur on the Pyr acceptor to NH for the DMPD group), and H_{ab} is the electronic coupling matrix element. We emphasize that the values for H_{ab} obtained by this procedure are highly approximate, given the poor resolution of the charge-transfer absorption features.

It was important to determine for comparison purposes whether CT interaction for Pyr and DMPD groups was indicated

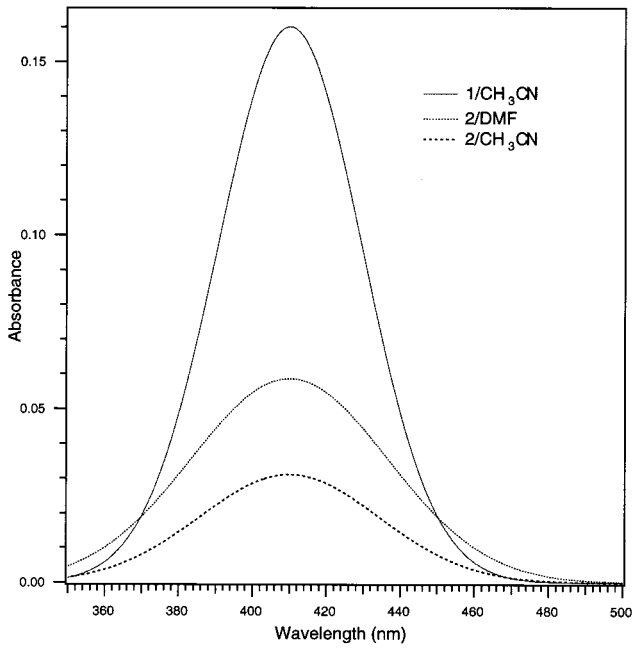

Figure 3. Absorption spectra in the long wavelength (charge transfer) region for **1** and **2**, obtained by subtraction of the spectrum for the reference pyrenesulfonyl derivative **5** from the absorption of the conjugates for solvents indicated.

in spectra for an *intermolecular* system. Complex formation could be detected for solutions of Pyr-AlaOEt (**5**) in the presence of the model electron donor, $CH_3CONHC_6H_4N(CH_3)_2$ (Ac-DMPD), again as a weak end absorption in the 400−430 nm range for acetonitrile solutions ranging in concentration up to 10 mM in **5** and Ac-DMPD. With the determination of an equilibrium constant ($K = 3.4 \times 10^3\ M^{-1}$) from data associated with the quenching of Pyr-AlaOEt fluorescence with Ac-DMPD,[20] it was possible to obtain an extinction coefficient for absorption by the complex ($\epsilon_{410} = 12\ M^{-1}\ cm^{-1}$, corresponding to $H_{ab} = 18\ cm^{-1}$). For this comparison, it was assumed that intermolecular complexation of Pyr-AlaOEt and Ac-DMPD results in formation of a conventional CT complex having a plane-parallel arrangement of the Pyr-AlaOEt and Ac-DMPD π systems.[16] The π-stack arrangement that is likely for **5** and Ac-DMPD is permissible (although not ideal) for Pyr-Ala-DMPD, but more probable for energetically allowed folded conformations of the longer peptides **3** and **4** (note discussion of models below). In contrast, the strongest evidence for CT interaction for the linear conjugates appears in the data for Pyr-DMPD (Figure 2) for which (plane parallel) π interaction is not possible. In addition, the CT contribution (Figure 3) falls off with the size of the linkage (**1** > **2** > **3**, **4**), *signaling further that the dominant mechanism of electronic coupling between terminal moieties in the ground electronic state is most likely to be through-σ-bonds*. This finding has been commonly made for linked donor−acceptor systems, including, for example, those featuring proline oligomers[2−4] and rigid hydrocarbon spacers.[21,22]

The fluorescence spectra for **2**−**5** are shown in Figure 4, and the quantum yields of emission for the conjugates are collected in Table 1. The emission spectral features for the DMPD derivatives were identical to that for **5**, which displays the fluorescence of the locally excited pyrenesulfonyl chromophore, having a vibronic progression of bands (ca. 900 cm^{-1}) and an origin at 390 nm. For the peptides in several solvents, longer wavelength emission that has been previously assigned to a mechanism of exciplex formation involving remotely attached

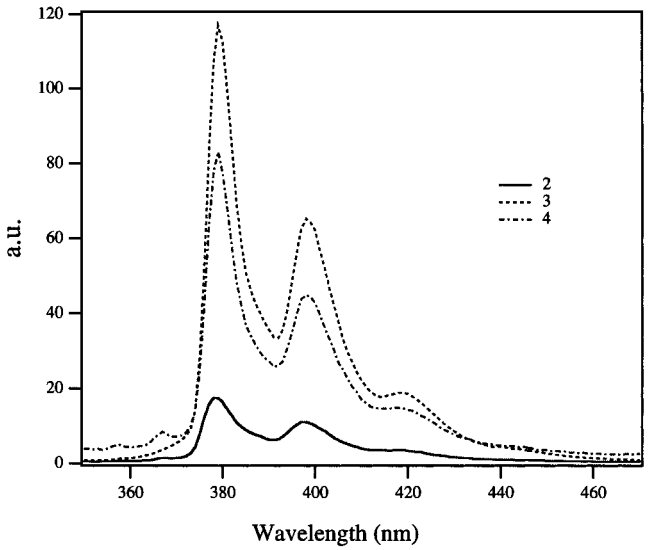

Figure 4. Fluorescence spectra for **2**−**4** in acetonitrile (25 μM samples; excitation at 337 nm).

TABLE 1: Fluorescence Quantum Yield and Transient Absorption Parameters for Pyrenesulfonamide Conjugates[a]

	Φ_f[b]	τ_1 (a_1)	τ_2 (a_2)	τ_3 (a_3)	τ_{av} (ps)
1	<0.0005	1.2 (1.0)			0.83
2	0.0045	9.7 (0.43)	53. (0.57)		43.1
3	0.024	13.5 (0.44)	60.9 (0.36)	1470 (0.20)	318
4	0.021	11.1 (0.37)	53.5 (0.39)	1530 (0.24)	379
5	0.83				

[a] Transient absorption for Ar-purged DMF solutions with lifetimes associated with 495 nm transient decays, τ_{1-3} (ps) values that result from single, double, and triple exponential fits with relative contributions, a_1-a_3, and a computed weighted average, τ_{av}. [b] Emission yield data for 25 μM Ar-purged CH_3CN solutions.

SCHEME 1

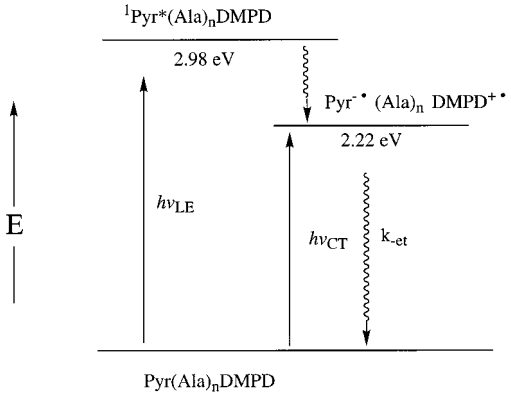

donor and acceptor groups in linked pyrene systems[23] has not been observed. Notably, the direct connection of Pyr and DMPD groups in **1** led to virtually complete quenching of Pyr fluorescence. Consistent with an electron transfer mechanism of quenching that is sensitive to the presence of spacer amino acid residues, fluorescence was substantially restored for the series of oligomeric peptides. However, values of emission quantum yield for peptides **3**−**5** fell in the same range and did not reveal a clear dependence on peptide chain length.[24,25] A model for the relative placement in energy of low-lying excited and radical-ion pair states that are accessible to the peptides is shown in Scheme 1. Used in this model are the energies derived from redox potential data obtained using cyclic voltammetry (Experimental Section) for the entries that serve as models lacking the peptide links, **5** and Ac-DMPD, and for **1**.

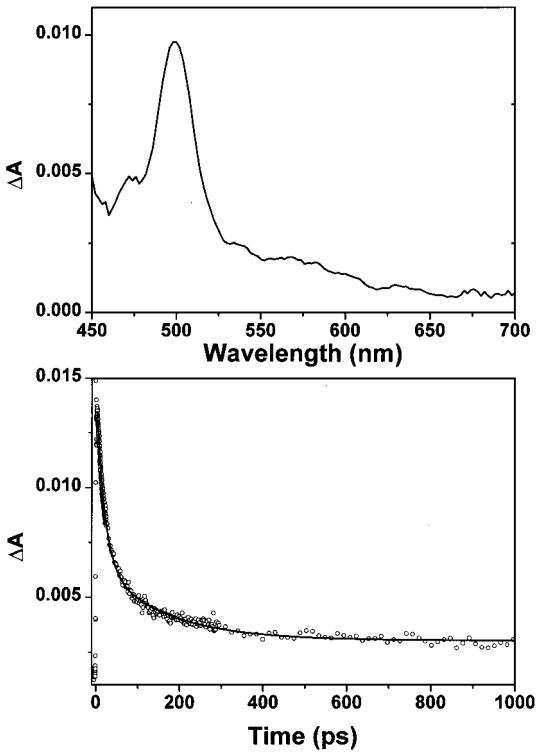

Figure 5. Transient spectrum (at 2.0 ps) and 495 nm transient decay curve obtained on pulsed laser photolysis of **3** in DMF (λ_{exc} = 400 nm).

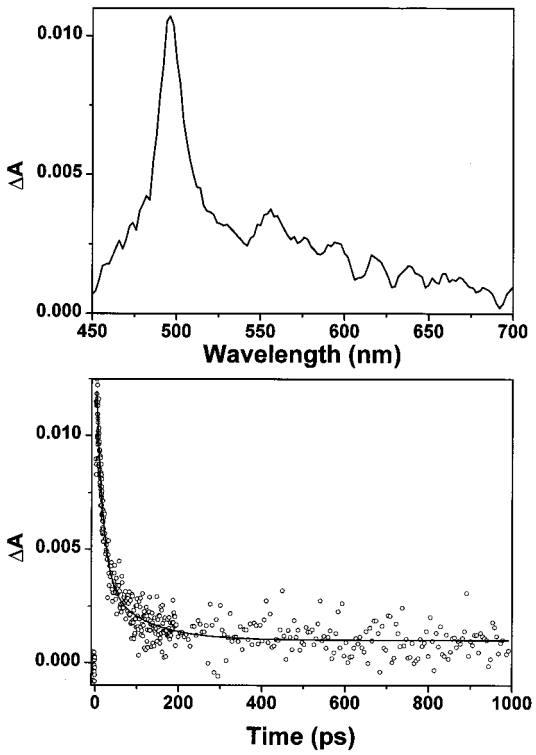

Figure 6. Transient spectrum (at 2.0 ps) and 495 nm transient decay curve obtained on pulsed laser photolysis of **4** in DMF (λ_{exc} = 400 nm).

Transient Absorption Properties of Peptide Conjugates. The events associated with formation and decay of electron transfer intermediates could be directly examined using femtosecond/picosecond transient absorption methods that employed laser excitation with a Ti/sapphire system capable of 70 fs pulses at the frequency-doubled wavelength (400 nm). For the reference conjugate, Pyr-AlaOEt, transient absorption was observed (λ_{max} = ca. 520, a band that was convoluted with stimulated emission) with an instrument-limited delay following laser pulse. The transient associated with **5** was long-lived (>10 ns), consistent with its identification with the fluorescent transient (the local Pyr S_1 state).[6,24]

On irradiation of the DMPD conjugates at 400 nm, a wavelength associated with the CT end absorption (Figure 2), a transient that grew in with the laser pulse (a rise time of ca. 300−600 fs) appeared with λ_{max} = 495 nm (Figures 5 and 6). This transient was assigned to the radical-anion of the pyrenesulfonyl moiety ($Pyr^{\bullet-}$), since it is similar in appearance to the absorption reported for the radical-anion of the parent hydrocarbon, pyrene (λ_{max} = 490 nm, ϵ = 49 200) and that of pyrene derivatives.[26] Transients also appeared to include weak absorption at longer wavelengths (a shoulder in the 520−560 nm range), consistent with the simultaneous appearance of the less strongly absorbing DMPD radical-cation transient, which has been observed in independent nanosecond flash photolysis experiments involving the model donor, Ac-DMPD.[27]

Decay times, assumed to represent the rates of charge recombination to the ground state (eq 3 and Scheme 1)[28] were obtained by monitoring the $Pyr^{\bullet-}$ transient at 495 nm for the series of Pyr conjugates (Table 1). The general pattern consisted of very rapid (1 ps) depletion for the directly linked **1** and a less rapid return electron transfer associated with longer links, **2**−**4**. The kinetics were complex, consistent with decay via back electron transfer for a multiplicity of species. For **2** a double exponential function was most suitable, whereas the data for the di- and tripeptides **3** and **4** were most satisfactorily fit to triple exponential functions that included a long τ component that reached the nanosecond regime. The decay data are organized in the table in terms of single and multiexponential lifetimes (τ_1−τ_3), along with a set of weighted averages, τ_{av}.

Molecular Modeling. The peptides selected for computer simulation were the alanine derivative **2** and the tripeptide, Pyr-Ala-Ala-Ala-DMPD (**4**), for which >500 local minima were inspected. The simulations provided comparisons of geometry and distance relationships for ensembles of the Pyr chromophore and the donor group, DMPD, and their energies relative to an arbitrary reference low-energy conformer. The distribution of conformations obtained for **4** is shown in Figure 7, which displays distributions of conformations in histogram form according to energy and critical distances. The average distances between putative electron donor and acceptor groups, defined in terms of through-space spans between points "center-to-center" for aromatic rings are 7.6 and 10. 2 Å, respectively for **2** and **4**; the respective through-bond distances "edge-to-edge" are 9.2 and 18.0 Å. The distribution of conformations for **4** is displayed in another way in terms of the distribution of dihedral angles made by main chain segments; these results are shown in the form of circle graphs (Figure 8).

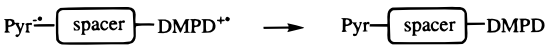

(3)

Discussion

In much of the important work to date regarding long-range electron transfer for synthetic peptide oligomers, the amino acid, L-proline, provides a relatively rigid link due to closure of the five-membered lactam ring (**6**). In the most extensive studies, Isied and co-workers[3] have deployed ruthenium, rhodium, and osmium transition metal complexes for terminal modification of proline oligomers. In these studies a charge shift process has

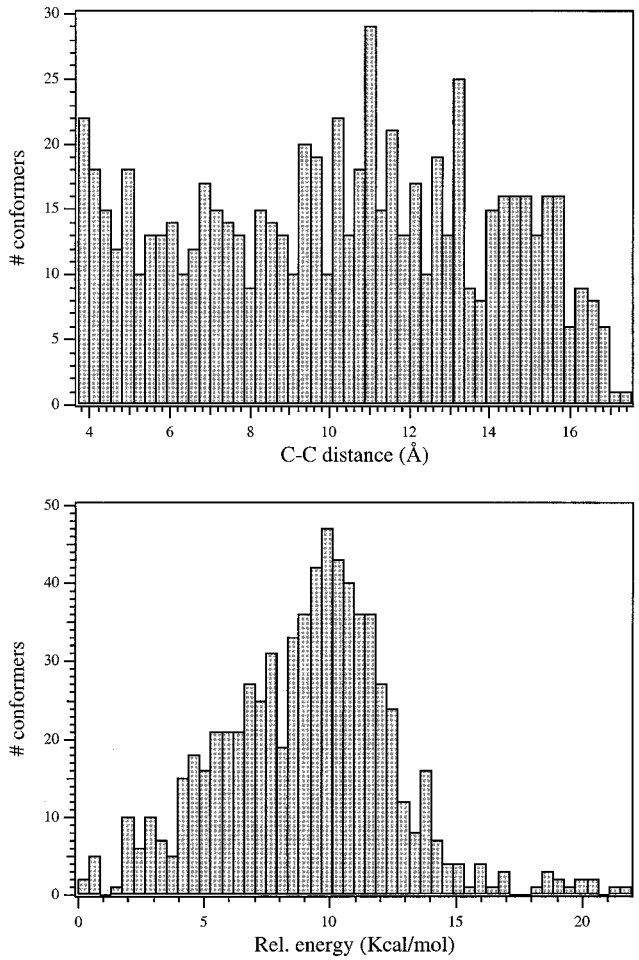

Figure 7. Molecular modeling results for **4** shown in histogram form that depict the distribution of 697 conformations with regard to the distance (center-to-center) of separation of Pyr and DMPD groups (top) and with regard to their relative energies (bottom).

been assessed (e.g., single electron transfer between Ru(I) and Ru(III) terminal groups, observed in pulse radiolysis experiments). Peptide oligomers that measure up to 40 Å in end-to-end separation of metal centers have been investigated with remarkable results that show that electron transfer can proceed over very long distances, albeit slowly (as low as k = ca. 10^4 s^{-1}) with moderate driving force, $\Delta G_{et} = -1.5$ eV. The most rapid of these electron transfers (for **6**, $n = 1$) occurs with a rate constant approaching 10^9 s^{-1}; the observation of a maintenance in electron-transfer rate for very long peptides in this series has been ascribed to the development of helical structure for the polyprolines for which additional electronic interaction between chain segments is important (vide infra).[3]

Other groups have employed spans of prolines separating organic donors and acceptors (e.g., tryptophan and tyrosine moieties, amino acid residues commonly found in proteins).[4] Using pulse radiolysis methods, Faraggi and Klapper[4] have surveyed oligomers with $n = 1-5$ with results that show a systematic falloff with the number of spacer residues. Rate constants associated with shifts of charge (hole or radical sites created at Trp moieties transferred to remotely placed Tyr) range 10^3-10^5 s^{-1}. Similar results have been provided by Bobrowski et al.,[4] regarding proline oligomer linkages of these amino acids. Mechanisms proposed to account for the rate constant trends have differed slightly for these two groups, with a through-bond electronic coupling mechanism cited in the work of Faraggi and Klapper[4] and a combination of mechanisms, through-bond at longer spacings of reactive residues and through-space interaction implicated for shorter links ($n = 1-3$), proposed by Bobrowski et al.[4]

Other investigations also address rates of end-to-end electron transfer across oligomer prolines, including the linked anthracene/dimethylaniline pairs of Maruyama et al.[29] and the connections of transition metal complexes with organic electron-transfer agents reported by Schanze and co-workers.[30] In another investigation by Fox and Miller,[31] radical-anion charge-shift reactions have been observed between organic groups that are linked, as in the present study, via alanine (Ala) residues. In these prior investigations, rates of electron transfer involving excited-state quenching or charge shift reach values of about 10^9 as an upper limit for short spans of amino acids ($n = 1-3$). Taken together these studies show that moderately large energy barriers for electron transfer remain for short links due to the influence of modest thermodynamic driving force or large reorganization energies.[32]

By any of these comparative measures, the rates of electron transfer (charge recombination, eq 3) for conjugates **1**−**4** are large. The trends in rate are expected to fall in the Marcus inverted regime (i.e., for the relationship of log k_{-et} and ΔG_{-et}[32]), since the thermodynamic driving force for charge recombination for these peptides is sizable (for the step, eq 3, $\Delta G_{-et} = -2.1$ eV). The inverted behavior is illustrated further by comparison with the series of similar tryptophan (Trp) conjugates that includes Pyr-Trp and Pyr-Ala-Trp,[6] derivatives that exhibit similar distance relationships vis-à-vis donors and acceptors as do **2** and **3**, respectively. Rates of charge recombination for the Trp series are about 1 order of magnitude slower than those associated with DMPD derivatives, in accord with *a higher driving force* for the Trp series (by about 0.5 eV).[6]

The interpretation of rate data for **1**−**4** must take into account the extensive conformational averaging that is important for these systems.[31] The modeling studies were carried out in order to confirm that peptide structures did not favor particular conformers based on some principle of long range ordering of the chains and pendant groups. Folded conformations, if favored, would introduce a mechanism of electron transfer that could be dominated by through-space interaction, if distances between electroactive pendants were as close as 5 Å.[8] For the peptide oligomers, a very large number of favorable conformations, representing, for **4**, distances of center-to-center separation of Pyr and DMPD groups of 8−15 Å, lie within a range of 5−7 kcal/mol in relative energy (>200 conformations in the simulation, Figure 7). The structural analysis for these conjugates that is in accord with 2D-NMR (NOE) findings[33] is one of peptide geometries in which the terminal groups (and chain segments) are oriented in largely random fashion, but with a large population of extended conformations (note the near random distributions of bond angles for d_3-d_6, d_8 for **4**, Figure 8). The simulations do not address the dynamics of such arrays, but a reasonable assumption is that conformational interconversions of significant dimensions are bounded in the microsecond to nanosecond time scale, as revealed in NMR and other studies of peptides.[34] Importantly, the dominant decay times for return electron transfer are very short, by comparison with this time scale for conformational averaging.

In sum, the behavior of the oligomers can be modeled simply in terms of a distribution of a large pool of random conformations into two families (Scheme 2). Some orientations that promote electronic coupling most effectively along peptide chains are associated with the weak CT absorption ($h\nu_{CT}$) that is observed for the series (Figure 2). This family of foldamers

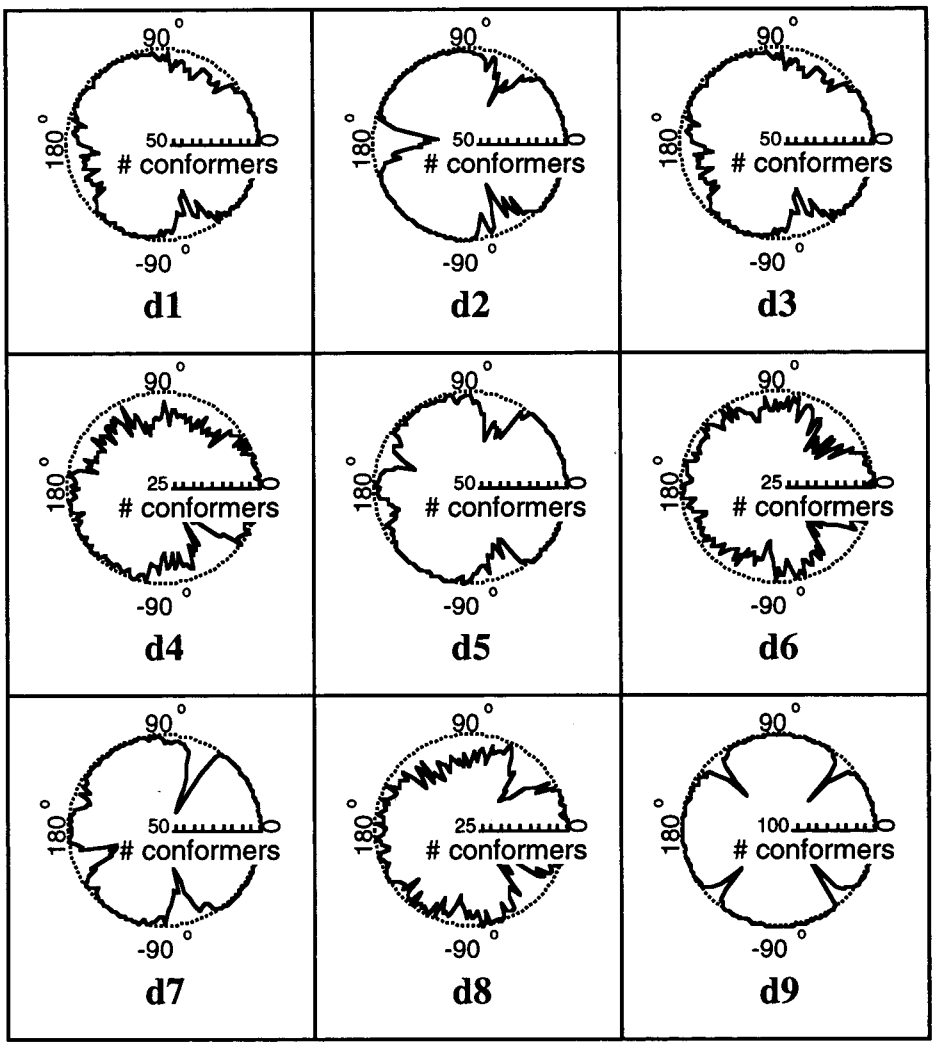

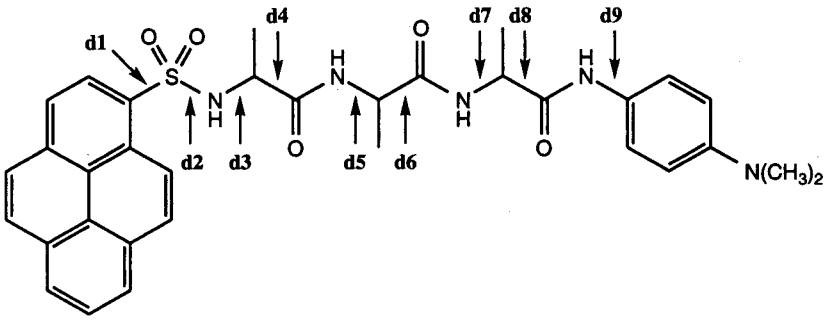

Pyr-Ala-Ala-Ala-DMPD

Figure 8. Distributions of conformations determined from simulations for **4** with reference to peptide backbone dihedral angles (reference structure shown).

is the source of the radical-ion phototransients that appear early in the picosecond time domain on laser photolysis at 410 nm and have decayed for the most part by 1 ns. These intermediates may be reasonably represented by the average distances of separation of Pyr and DMPD groups indicated in the simulation (e.g., about 7 and 11 Å for **2** and **4**, respectively), corresponding roughly to solvent-separated radical-ion pairs.[17,32]

As the result of a random sampling of peptide backbone and other angles, a second family of peptide conformations is less suited for long-range interaction via through-bond (or through space) electronic coupling. Following photoexcitation associated with local pyrene absorption ($h\nu_{LE}$, ca. 330 nm), these species survive well into the mampsecpmd regime and are responsible for normal Pyr fluorescence. The implication is that the majority of these species undergo forward electron transfer on a time scale that is slower than that associated with the rates of return of radical-ion pairs to the ground state; the two distinguishable slow and fast processes (eqs 1 and 3) represent behavior associated with normal and inverted Marcus regimes, respectively.

SCHEME 2

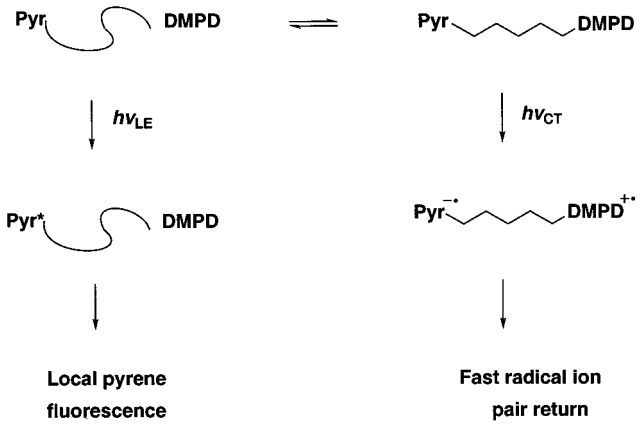

The feature of the kinetics data that remains is the dependence of charge recombination rate on peptide length. A falloff in transient decay times with the number of intervening amino acids is clearly apparent for **1**−**3**; although not having precise physical meaning, average rate constants for return electron transfer (i.e., the reciprocal average decay times) are, respectively, 12×10^{10}, 2.3×10^{10}, and 0.31×10^{10} M^{-1} s^{-1}. It is tempting to record simply that the trend shows a regular dependence of a near 10-fold decrease in rate with the imposition of each Ala spacer (3 σ bonds or about 4.5 Å). The standard view[8,21] is that the charge recombination rate constant should be related to H_{ab} and the Franck−Condon weighted density of states (FCWD) for electron transfer and that the electronic coupling term scales exponentially with distance with coefficient $-\beta$ (eqs 4 and 5). For the series **1**−**3**, the computed β value is

$$k_{et} = 4\pi^2/h|H_{ab}|^2\text{FCWD} \quad (4)$$

$$|H_{ab}|^2 = |H_{ab}(\text{max})|^2 \exp(-\beta r_{DA}) \quad (5)$$

0.22, an indicator of very effective electronic coupling for these short links, but a number that is based on the simplest assumed distance relation. For comparison, the range of β values observed for oligoproline linked D−A systems is 0.2−1.0 $Å^{-1}$.[3,4]

That the real distance dependence for this series is more complicated is clear on comparing di- and tripeptides, **3** and **4**. Within the error limits of the decay time experiments, these two peptides behave in a remarkably similar fashion in terms of quantum yields of fluorescence and radical-ion-pair decay times. Several factors could be at play in the assistance to charge recombination for the longer peptide **4**. According to the Marcus−Hush semiclassical theory,[8,32] the solvent reorganization energy (λ_{out}) that is approximated by the dielectric continuum model is a subtle function of distance. According to Liang and Newton,[35] this parameter is predicted to show a weaker dependence on donor−acceptor separation for electron transfer *in the inverted region*.[36]

Another potential influence for the present series is the "harpoon" mechanism proposed by Verhoeven et al.,[37] under which the average through-space distance between end groups is influenced by electrostatic attraction, a feature that requires more conformational freedom (i.e., linked ion pairs are driven to favorable distances for charge recombination for the longer peptide). This kind of mechanism will, however, depend to a degree on the time scale of the Brownian motion of chain ends for peptide oligomers. Some sense of this time scale is provided in a study of energy transfer between naphthalene and (dimethylamino)naphthylsulfonyl (dansyl) chromophores across a flexible chain of hydroxyethylglutamines.[38] The estimates of relative diffusion coefficients for chain ends that were derived in this study resulted from emission lifetime data that fell in the 5−15 ns range for the shortest oligomers examined ($n = 4$, 5), a time scale that is long relative to the present findings of charge recombination times for the oligomers, **2**−**4**.[39] That is, the values of average k_{-et} are too large to be influenced significantly by a conformational gating that is at least partially rate limiting (i.e., the charge recombination rates reflect the behavior of a relatively static ensemble). Finally, the role of partially folded peptide chains has received special scrutiny in terms of specific modes of electronic coupling via hydrogen bonding.[40] For example, in command of more conformational space, the tripeptide **4** will have increased opportunity to participate in specific intramolecular H-bond patterns that may amplify the usual through (peptide) σ bond coupling mechanism.

Acknowledgment. Support of this research by the Department of Energy, Office of Basic Energy Sciences, Division of Chemical Sciences, is gratefully acknowledged. We also wish to thank Xin Zhou and Valentine Vullev for technical assistance.

References and Notes

(1) Paper no. 9 from Boston University in the series *Photoactive Peptides*.

(2) Isied, S. S. In *Principles of Electron-Transfer Reactions: Applications in Inorganic and Organometallic Chemistry and Biology*; Isied, S. S., Ed.; Advances in Chemistry Series 253; American Chemical Society: Washington, DC, 1997. Slate, C. A.; Striplin, D. R.; Moss, J. A.; Chen, P.; Erickson, B. W.; Meyer, T. J. *J. Am. Chem. Soc.* **1998**, *120*, 4885.

(3) Ogawa, M. Y.; Moreira, I.; Wishart, J. F.; Isied, S. S. *Chem. Phys.* **1993**, *176*, 589. Mishra, A. K.; Isied, S. S.; Ogawa, M. Y.; Wishart, J. F. *Chem. Rev.* **1992**, *92*, 381.

(4) Chandrasekar, R.; Faraggi, M.; Klapper, M. H. *J. Am. Chem. Soc.* **1994**, *116*, 1414. DeFelippis, M. R.; Faraggi, M.; Klapper, M. H. *Ibid.* **1990**, *112*, 5640. Bobrowski, K.; Holcman, J.; Poznanski, J.; Ciurak, M.; Wierzchowski, K. L. *J. Phys. Chem.* **1992**, *96*, 10036.

(5) Fox, M. A.; Galoppini, E. *J. Am. Chem. Soc.* **1997**, *119*, 23; **1996**, *118*, 2299. Werner, U.; Wiessner, A.; Kuehnle, W.; Staerk H. *J. Photochem. Photobiol. A: Chem.* **1995**, *85*, 77. Mihara, H.; Tanaka, Y.; Fujimoto, T.; Nishino, N. *J. Chem. Soc., Perkin Trans. 2* **1995**, 1915; *Chem. Lett.* **1996**, 135. Garcia-Echeverria, C. *J. Am. Chem. Soc.* **1994**, *116*, 6031. Sisido, M.; Tanaka, R.; Inai, Y.; Imanishi, Y. *Ibid.* **1989**, *111*, 6790. Sisido, M.; Inai, Y.; Imanishi, Y. *Macromolecules* **1990**, *23*, 1665. Tamiaki, H.; Maruyama, K. *Chem. Lett.* **1993**, 1499.

(6) Jones, G., II; Lu, L. N.; Vullev, V.; Gosztola, D. J.; Greenfield, S. R.; Wasielewski, M. R. *Bioorg. Med. Chem. Lett.* **1995**, *5*, 2385. Jones, G., II; Feng, Z.; Oh, C. *J. Phys. Chem.* **1995**, *99*, 3883. Jones, G., II; Farahat, C. W.; Oh, C. *Ibid.* **1994**, *98*, 6906. Jones, G., II; Farahat, C. W. *Res. Chem. Intermediates* **1994**, *20*, 855.

(7) Jones, G., II; Lu, L. N. *J. Org. Chem.* **1998**, *63*, 8938.

(8) Newton, M. *Adv. Chem. Phys.* in press. Beratan, D. N.; Onuchic, J. N. Chapter 2 in ref 9. Onuchic, J. N.; De Andrade, P. C. P.; Beratan, D. N. *J. Chem. Phys.* **1991**, *95*, 1131; **1990**, *92*, 722.

(9) Bendall, D. S., Ed. *Protein Electron Transfer;* BIOS Scientific Publishers Ltd.: Oxford, U.K., 1996.

(10) Kozlov, G. V. Ogawa, M. Y. *J. Am. Chem. Soc.* **1997**, *119*, 8377. McLendon, G. L.; Wishart, J. F.; Baillard, E. R.; Corin, A. F. *Proc. Natl. Acad. Sci. U.S.A.* **1996**, *93*, 9521. Rabanal, F.; DeGrado, W. F.; Dutton, P. L. *J. Am. Chem. Soc.* **1996**, *118*, 473.

(11) Lloyd-Williams, P.; Albericio, F.; Giralt, E. *Chemical Approaches to the Synthesis of Peptides and Proteins*; CRC Press: Boca Raton, FL, 1997; Bodanszky, M. In *Principles of Peptide Synthesis*, 2nd ed.; Springer-Verlag: New York, 1993.

(12) Ezzell, S. A.; McCormick, C. L. *Macromolecules* **1992**, *25*, 1881.

(13) Jones, G., II; Oh, C. *J. Phys. Chem.* **1994**, *98*, 2367.

(14) Wynne, K.; Reid, G. D.; Hochstrasser, R. M. *Opt. Lett.* **1994**, *19*, 895.

(15) Clark, T. In *Handbook of Computational Chemistry*; John Wiley: New York, 1985.

(16) Foster, R. *Organic Charge-transfer Complexes*; Academic Press: New York, 1969.

(17) Jones, G., II. In *Photoinduced Electron Transfer, Part A*; Fox, M. A., Chanon, M., Eds.; Elsevier: New York, 1988.

(18) Hush, N. S. *Coord. Chem. Rev.* **1985**, *64*, 135. Mulliken, R. S. *J. Am. Chem. Soc.* **1952**, *64*, 811.

(19) Creutz, C.; Newton, M. D.; Sutin, N. *J. Photochem. Photobiol. A: Chem*. **1994**, *82*, 47.

(20) A Stern−Volmer plot of fluorescence quenching of **5** by AcDMPD provided a value for the slope of 3.4×10^3 M^{-1}; given a fluorescence lifetime for **5** in DMF of 20 ns, a rate constant for bimolecular quenching of 1.7×10^{11} M^{-1} s^{-1} is computed. Since the latter value is well above that assumed for diffusion-limited quenching, a static quenching mechanism is required (i.e., ground-state CT complexation).

(21) Curtiss, L. A.; Naleway, C. A.; Miller, J. R. *J. Phys. Chem*. **1995**, *99*, 1182. Jordan, K. D.; Paddon Row, M. N. *Chem. Rev*. **1992**, *92*, 395. Shephard, M. J.; Paddon-Row, M. N.; Jordan, K. D. *Chem. Phys*. **1993**, *176*, 289.

(22) For examples and leading references regarding through-bond intramolecular CT systems, see: Verhoeven, J. W.; Wegewijs, B.; Scherer, T.; Rettschnick, R. P. H.; Warman, J. M.; Jaeger, W.; Schneider, S. *J. Phys. Org. Chem*. **1996**, *9*, 387. Penfield, K. W.; Miller, J. R.; Paddon-Row, M. N.; Cotsaris, E.; Oliver, A. M.; Hush, N. S. *J. Am. Chem. Soc*. **1987**, *109*, 5061.

(23) See, for example: Petrov, N. Kh.; Borisenko, V. N.; Alfimov, M. V.; Tiebig, T.; Staerk, H. *J. Phys. Chem*. **1996**, *100*, 6368. Cao, H.; Fujiwara, Y.; Haino, T.; Fukazawa, Y.; Tung, C. H.; Tanimoto, Y. *Bull. Chem. Soc. Jpn*. **1996**, *69*, 2801.

(24) Average fluorescence decay times for **3**−**5** range 6−20 ns; further details regarding fluorescence properties of the conjugates for various solvents will be separately reported.[25]

(25) Jones, G., II; Zhou, X.; Lu, N. L.; Fu, H. Manuscript in preparation.

(26) Grellman, K. H.; Watkins, A. R.; Weller, A. *J. Lumin*. **1970**, *12*, 678. Lianos, P.; Georghiou, S. *Photochem. Photobiol*. **1979**, *29*, 13.

(27) In nanosecond flash photolysis experiments involving electron-transfer quenching of the quinone oxidant, chloranil triplet, the radical-cation of Ac-DMPD has been observed as a broadly absorbing transient with $\lambda_{max} = 550$ nm and $\epsilon_{550} =$ ca. 9500 M^{-1} cm^{-1} Farahat, C. W. Ph.D. Dissertation, Boston University, 1992, Chapter 3.

(28) An alternate mechanism of charge recombination (formation of singlet radical-ion pairs followed by decay, not to the ground state, but to a local triplet) has been established in a separate nanosecond flash photolysis study of Pyr-modified Ala oligomers containing electron donor tryptophans (Trp);[7] e.g., for Pyr-Ala-TrpOEt, formation of local triplet states of Pyr was observed in the microsecond time domain, a result not obtained for the present Pyr/DMPD series, consistent with the relative positioning in energy of radical-ion pairs for the latter slightly below the Pyr triplet.

(29) Tamiaki, H.; Maruyama, K. *J. Chem. Soc., Perkin Trans. 1* **1991**, 817.

(30) Schanze, K.; Cabana, L. A. *J. Phys. Chem*. **1990**, *94*, 2740.

(31) Fox, M. A.; Miller, J. R. *J. Org. Chem*. **1991**, *56*, 5380.

(32) Kavarnos, G. J. *Top. Curr. Chem*. **1990**, *156*, 23.

(33) Jones, G., II; Lu, N. L.; Mari, F. Manuscript in preparation.

(34) Wright, P. E. *Annu. Rev. Biophys. Biophys. Chem*. **1991**, *20*, 519. Cummings, A. L.; Eyring, E. M. *Biopolymers* **1975**, *14*, 2107.

(35) Liang, C.; Newton, M. D. *J. Phys. Chem*. **1993**, *97*, 3199.

(36) Using the dielectric continuum treatment, solvent reorganization energies fall in the range, $\lambda_{out} = 0.83-1.10$ eV (DMF solvent) for through-space distances of Pyr/DMPD separation of 8.0−12.0 Å.

(37) Lauteslager, X. Y.; Wegewijs, B.; Verhoeven, J. W.; Brouwer, A. M. *J. Photochem. Photobiol. A* **1996**, *98*, 121.

(38) Haas, E.; Katchalski-Katzir, E.; Steinberg, I. Z. *Biopolymers* **1978**, *17*, 11.

(39) An interesting finding of the energy transfer study[38] is that the relative rate of diffusive motion for chain ends is increasingly inhibited for *shorter* peptide links.

(40) Kurnikov, I. V.; Zusman, L. D.; Kurnikova, M. G.; Farid, R. S.; Beratan, D. N. *J. Am. Chem. Soc*. **1997**, *119*, 5690, and references cited therein.